RSC Pharmaceutics

ROYAL SOCIETY OF CHEMISTRY

PAPER

View Article Online
View Journal

Cite this: DOI: 10.1039/d6pm00029k

PLGA and Eudragit-based long-acting microspheres for Parkinson's disease management

Deepa D. Nakmode, Haripriya Koppisetti, Weranga Rajapaksha, Yunmei Song and Sanjay Garg *

Oral medications available for Parkinson's disease require multiple administrations, which significantly affects the plasma concentration of the drug, and patients struggle to adhere to the treatment regimen due to the complexity of frequent dosing. Therefore, the idea of developing a long-acting biodegradable microsphere formulation was adopted. The biodegradable microspheres were prepared using a combination of $PLGA_{50:50}$ and Eudragit L-100. This combination incorporates the advantages of both $PLGA_{50:50}$ and Eudragit L-100 to achieve optimum drug release. The drug loaded was pramipexole. Since pramipexole is hydrophilic in nature, microspheres were fabricated using a double emulsion solvent evaporation process. The optimized microsphere formulation demonstrated an initial burst release of up to 24.18%, followed by a slow release of pramipexole for up to 18 days (93.78%) without the need to convert the drug into its salt form. The *ex vivo* drug release showed 78.96% release of pramipexole in 10 days. The optimized microspheres were further studied by DSC, FTIR, NMR, and SEM. The syringeability analysis of the microspheres, when suspended in sodium CMC solution, demonstrated an injectable force of 3.25 ± 0.24 N.

Received 22nd January 2026,
Accepted 8th June 2026

DOI: 10.1039/d6pm00029k

rsc.li/RSCPharma

Introduction

The treatment strategies for Parkinson's disease have developed considerably in recent years. Pharmacological therapies, including levodopa, dopamine receptor agonists, anticholinergic agents, monoamine oxidase B (MAO-B) inhibitors, and catechol-*O*-methyltransferase (COMT) inhibitors, remain the basis of symptomatic management and are widely reviewed in clinical practice.[1]

Levodopa is always given in combination with carbidopa to prevent its systemic adverse effects. Along with carbidopa, another class of drugs, COMT inhibitors (tolcapone and entacapone), has been added to the treatment regimen. They are approved for patients experiencing "wearing-off" phenomena, where the effect of levodopa diminishes before the next dose.[2] Despite the well-established efficacy of levodopa as the most potent symptomatic treatment, increasing emphasis has been placed on "levodopa-sparing strategies" in early Parkinson's disease. These approaches aim to delay the onset of long-term motor complications, particularly motor fluctuations and dyskinesias, which are strongly associated with chronic levodopa exposure and pulsatile dopaminergic stimulation. Another class of drugs, dopamine receptor agonists, mimics the natural action of dopamine and works by direct stimulation of dopamine receptors.[1] Pramipexole and ropinirole are among the most frequently used dopamine agonists; pramipexole tends to be more potent.[1]

Pramipexole belongs to the non-ergot dopamine agonist class, which was first introduced in 1997 in the US, followed by European countries. It is currently prescribed as monotherapy and as adjunctive therapy with levodopa.[3] In early-stage Parkinson's disease, pramipexole can be prescribed as monotherapy, which delays the need for levodopa.[4] Pramipexole is a synthetic non-ergot, aminothiazole dopamine agonist with affinity for dopamine D_2 and D_3 receptors.[5–8] The higher affinity of pramipexole for the D_3 receptor[5] contributes to its efficacy against the psychiatric symptoms of Parkinson's disease, such as depression.[9] Pramipexole is presently available in the market as an oral immediate-release tablet, which is administered 3 times a day.[10–12] The current immediate-release tablet formulation of pramipexole requires administration 3 times a day, resulting in fluctuations in the plasma concentration of pramipexole.[10] Clinical studies demonstrate that pramipexole is effective both as monotherapy in early-stage Parkinson's disease and as an adjunct to levodopa in advanced stages. In addition to improving motor symptoms such as akinesia, rigidity, and resting tremor, pramipexole has also been shown to alleviate depressive symptoms. It is generally well

Centre for Pharmaceutical Innovation (CPI), College of Health, Adelaide University, Adelaide, SA 5000, Australia. E-mail: sanjay.garg@adelaide.edu.au; Tel: +61-8-8302-1575

tolerated; however, compared with levodopa, it is associated with a higher incidence of certain dopaminergic adverse effects.[3]

Pramipexole is well absorbed when given orally;[13] however, it still requires multiple administrations due to its short half-life. Additionally, many patients experience dysphagia with oral medication.[14] To address these limitations, a sustained-release formulation is needed, which will enable slow release of the drug for a longer time. Long-acting injectables can be used as an alternative option, which will reduce the need for multiple administrations.

The design of a long-acting formulation depends on the physicochemical properties of the API including molecular weight, log *P*, solubility, and hydrophobicity. In addition, safety, therapeutic area, administration needs, pharmacokinetics, and pharmacodynamics of the API are crucial factors in the design of the long-acting formulation.[15] Multiple methods of controlling release duration have been developed as a result of the range of potential drug features and applicable disorders. Numerous drug delivery systems, including microencapsulation,[16,17] oil-based solutions and suspensions,[18,19] *in situ* forming implants,[20,21] nanocrystal suspension,[22] long-acting hydrogels, long-acting microneedles,[23] and long-acting implants,[24] have been developed to maintain drug release.[25] Based on the physicochemical data, pramipexole is highly hydrophilic in nature, so controlling the release of hydrophilic drugs requires encapsulation of the drug or conversion into a less soluble pro-drug form. Nevertheless, for hydrophilic drugs, a microsphere formulation is the best approach for sustaining drug release due to its flexibility in modifying drug release.[26] In addition, microspheres can increase the efficiency and the duration of action of drugs, along with the prevention of drug degradation after administration. Different strategies for encapsulation are applied according to the drug's solubility and inherent properties.[27] For example, solvent evaporation, oil-in-water (o/w) emulsion for hydrophobic drugs, and water-in-oil-in-water (w/o/w) double emulsion for water-soluble drugs are employed.[27–29]

Various pramipexole formulations have been developed by researchers. For example, in 2018, Raj *et al.*[30] formulated pramipexole dihydrochloride loaded nanoparticles for nose-to-brain delivery of pramipexole. However, the *in vitro* release and *ex vivo* studies showed drug release for up to 24 hours. Hence, this formulation cannot be used for achieving sustained drug release for a longer period. In 2023, Pamlenyi *et al.*[31] developed pramipexole-loaded buccal films for improving the absorption of the drug. The *in vitro* release showed up to 80% drug release in 20 minutes.

The literature on pramipexole long-acting formulations includes a study by Li *et al.*, 2019,[32] which reported a near-infrared light-responsive microsphere for pramipexole; however, this formulation requires external light stimulation to achieve drug release, which reduces its practicality for continuous use. Another study by Ban *et al.*, 2025,[33] involves the conversion of pramipexole into its xinafoate salt form, which adds a layer of manufacturing complexity. Additionally, the xinafoate salt form has not been approved by the FDA for injectables to date.

In this study, we explored the double emulsion (W/O/W) solvent evaporation method for pramipexole microsphere preparation using a combination of polymers, namely PLGA and Eudragit L-100. This method is simple compared to the tedious method of converting the drug into a lipophilic form, which adds to the complexity of scale-up. This is the first study to discuss long-acting injectable microspheres for pramipexole using a combination polymer, PLGA and Eudragit L-100. The optimized microspheres were also characterized for *in vitro* drug release, drug loading, encapsulation efficiency, syringeability, viscosity, XRD, DSC, and particle size distribution.

Materials and methods

Materials

$PLGA_{50:50}$ (inherent viscosity 0.17 dl g^{-1}, acid terminated) was obtained from Nomisma Healthcare (Gujarat, India). Polyvinyl alcohol (87–90% hydrolysed, MW: 30 000–70 000) was procured from Sigma (the Netherlands). Sodium phosphate dibasic was purchased from Sigma (Germany). Potassium phosphate monobasic, Tween 80 and dimethyl sulfoxide (DMSO) were procured from Chemsupply (Gillman, Australia). Ethyl acetate was procured from Merck (South Africa). Dichloromethane was purchased from Sigma-Aldrich (MO, USA). Eudragit L-100 was procured from Evonik (Darmstadt, Germany). Acetonitrile was obtained from Sigma-Aldrich (NSW, Australia). Pramipexole was acquired from BLD Pharma Tech Ltd (China).

Quantification of pramipexole by the HPLC method

The analysis of the release samples was carried out using an HPLC system (Shimadzu Corporation, Kyoto, Japan), a quaternary pump (LC-20AD), a degasser (DGU-20A3), an autosampler (SIL-20A HT), and a single-channel ultraviolet (UV) detector (SPD-20A). The Luna C18 column (250 × 4.6 mm, 5 μm), manufactured by Phenomenex, was used as the stationary phase. For processing the data, LabSolutions (version 5.92) software developed by Shimadzu Corporation was utilised. The high-performance liquid chromatography (HPLC) method was adapted from the literature[34] with some modifications, and validation was performed for the analysis of release samples and drug-loading samples. The optimized method conditions were a flow rate of 1 mL min^{-1} and UV detection at 264 nm; the injection volume was set to 10 μl, and the temperature of the column was 40 °C. Gradient elution was performed using mobile phase A, consisting of solution A, prepared by adding 9 grams of monobasic potassium phosphate and 2 grams of sodium 1-octanesulfonate anhydrous (pH adjusted to 3 using phosphoric acid), and mobile phase B, containing acetonitrile : solution A 50 : 50. The optimised gradient elution is detailed in Table 1. The run time was set to 12 minutes, with pramipexole eluting at 7.74 min.

Table 1 Optimised HPLC gradient

Time (min)	Mobile phase A (%)	Mobile phase B (%)
0	60	40
10	20	80
12	60	40

Preparation of microspheres

Firstly, a polymeric solution of PLGA and Eudragit L 100 was prepared with an ethyl acetate : DMSO mixture (1 : 2) at 35 °C. The drug (60 mg in all formulations) was dissolved in the water phase (W_1) containing an emulsifier (1% PVA) and then dispersed into the polymer solution in an organic solvent (O) with stirring to prepare the primary W_1/O emulsion. Secondly, this W_1/O emulsion was emulsified in a large volume of the external aqueous phase containing an emulsifier (W_2), in which the polymer is insoluble. The emulsion was stirred overnight to evaporate the organic solvent, and drug-loaded microspheres were formed after solvent evaporation. The precipitation of the polymer occurs upon encapsulation of the internal drug phase and evaporation of the organic solvent. The prepared microspheres were washed with Milli-Q water, and the supernatant was separated by centrifugation and freeze-dried for 48 hours (Fig. 1).

Characterisation of microspheres

Drug loading and encapsulation efficiency. Entrapment efficiency (EE) helps in determining the amount of drug encapsulated in the microspheres. For evaluating the entrapment efficiency, 10 mg of microspheres were dissolved in dichloromethane (1 ml) and bath sonicated, followed by the addition of 0.1 N phosphoric acid. The supernatant was passed through a 0.45 μm filter, and the filtrate was analysed by HPLC. The EE of the microspheres was calculated using the following formula.[35]

$$\mathrm{EE} = \frac{\text{amount of drug in microspheres}}{\text{total amount of drug added}} \times 100$$

Meanwhile, the % drug loading was calculated using the following formula.

$$\mathrm{DL} = \frac{\text{amount of drug in microspheres}}{\text{total amount of drug + polymer added}} \times 100.$$

***In vitro* drug release study.** The dialysis bag method was utilized for the *in vitro* drug release study.[36] For this study, ~100 mg of drug-loaded microspheres was added to a dialysis bag sealed at one end with 1 ml of pH 7.4 phosphate buffer, and the other end was sealed. The dialysis bag was dispersed in pH 7.4 phosphate buffer (10 ml) with 0.1% Tween 80 in a 20 ml glass vial. All the release samples were transferred to a 37 °C incubator set at 250 rpm. At predetermined time points, samples were withdrawn, and the release media were completely replaced with fresh buffer for maintaining sink conditions. The collected release samples were filtered *via* 0.45 μm syringe filters and stored at −20 °C until analysis by HPLC.

Mathematical modelling of the drug release profile. To evaluate the mechanism by which pramipexole was released from the microsphere formulation, various mathematical models were applied to the *in vitro* release data. The following criteria were applied for evaluating the goodness of fit, the adjusted R^2, and the Akaike information criterion (AIC).[37]

Particle size distribution. A Mastersizer 3000 (Malvern Instruments Ltd) was used for the particle size distribution (PSD) analysis of the microspheres. For the PSD analysis, freeze-dried microspheres were suspended in 400 mg of Milli-Q water until the obscuration reached 1–6%. The mean size D_{50}, D_{90}, and span index were recorded. The span index of the

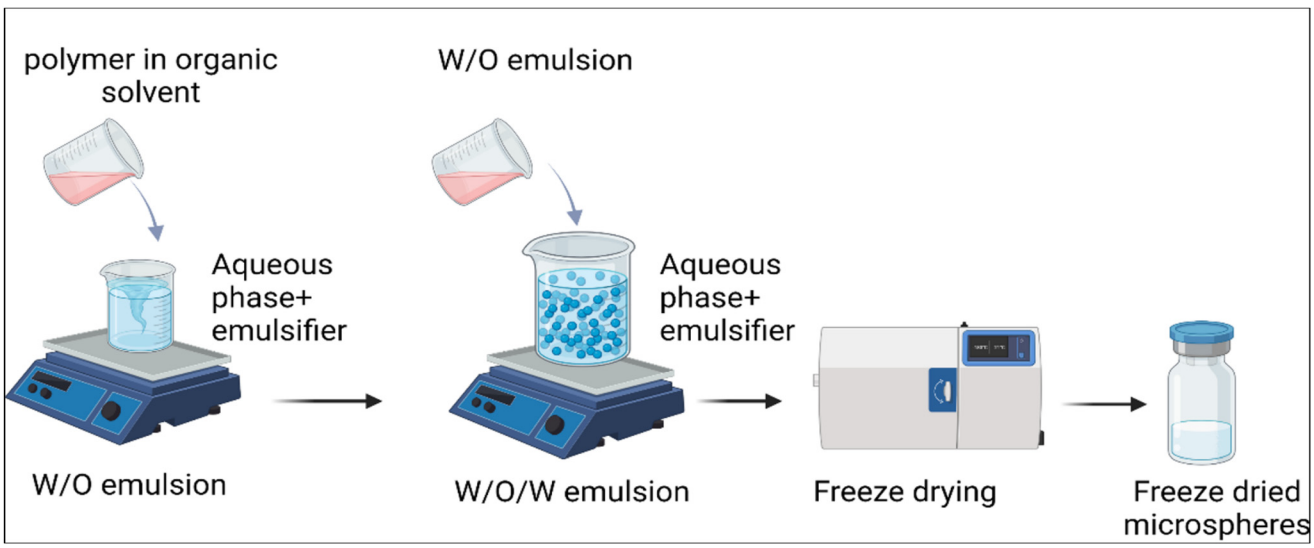

Fig. 1 Diagrammatic representation of the double emulsion solvent evaporation technique (created using BioRender).

optimized microspheres was determined using the following equation:

$$\text{Span index} = (D_{90} - D_{10})/D_{50}$$

D_{90}, D_{50}, and D_{10} values were obtained from the Mastersizer and refer to the particle sizes at which 90%, 50%, and 10% of the particles fall within the cumulative particle size distribution.

Scanning electron microscopy (SEM). The morphology of the prepared microspheres was assessed using scanning electron microscopy (Zeiss Merlin FEG SEM). For studying changes in surface morphology during the *in vitro* drug release, microspheres were collected at different time points and freeze-dried. Microspheres suspended in RO water were placed on a stub, which was air-dried at room temperature. All the samples were coated with platinum using an Agar high-resolution sputter coater. The morphology of the coated samples was then examined using SEM.

Differential scanning calorimetry (DSC). The prepared microspheres were evaluated for thermal properties by DSC. The microspheres, which were prepared by double emulsion, were observed for changes in the mass at the boiling point of the organic solvent used for the preparation of those microspheres, which gives an idea about the complete evaporation of the organic solvent from the microspheres.[38] The DSC curve for the microspheres helps identify if there is any change in the polymorphic form of the drug or polymer.

Fourier transform infrared (FTIR) spectroscopy. Analysis was performed using an FTIR spectrometer (Bruker, Massachusetts, USA) for studying the drug and polymer interaction. For the analysis, a small amount of sample was positioned on the ATR diamond crystal, with a clamp used to maintain consistent contact of the sample with the crystal. All the measurements were performed in transmittance mode from 4000 to 450 cm^{-1} with 16 scans per sample at room temperature.

PCA of FTIR spectra. Principal component analysis (PCA) has been applied to identify the patterns and relationships between the examined samples. The table was created using samples as observations (rows) and wavenumbers as features (columns) by rearranging the original table.[39] To highlight the shape[40] differences, features were mean-centred and unit variance scaled before PCA. RStudio was used for performing PCA on the standardized dataset using singular value decomposition. Plots of PC1 *vs.* PC2 scores were generated.

Proton nuclear magnetic resonance (NMR). For proton NMR analysis, 5 mg of the sample (pramipexole, PLGA, and microspheres) was solubilised in 0.35 mL of deuterated dimethyl sulfoxide, and the solutions were transferred to NMR tubes. All the proton measurements were performed using a Bruker Avance III HD spectrometer (Bruker Corporation, Faellanden, Switzerland) at 500 MHz and were analyzed using the NMRium program. The chemical shifts were presented in parts per million (ppm) and were referenced to ^{1}H signals of residual non-deuterated solvent.[41]

X-Ray diffraction (XRD). XRD analysis of the drug, a physical mixture of the polymer and drug, and the prepared microspheres was carried out to study the nature of the drug before and after entrapment of the drug into the microspheres. If there is an alteration in the drug's polymorphic form or polymers, it can be easily detected by XRD. The XRD patterns for the samples were recorded using a Rigaku MiniFlex 600 instrument, with Cu Kα radiation at 40 kV and 15 mA. The diffraction angle for the analysis (2θ) ranges from 10° to 90°.

Viscosity studies. The viscosity of the suspended microspheres was evaluated using a Rheosys Merlin VR (Scientex Pty Ltd, Melbourne, Victoria, Australia). A parallel plate with a diameter of 30 mm and a gap of 0.5 mm was used. The viscosity values were plotted against the corresponding shear rate (s^{-1}).

Sedimentation volume determination. For evaluating the sedimentation of the suspended microspheres, the sedimentation volume was determined for up to 24 hours without disturbing the samples.[42] The sedimentation volume was recorded as the ratio of the ultimate settled height (H_u) to the original height (H_0) as shown in the equation below. For measuring sedimentation volume, 500 mg of microspheres were suspended in 5 ml of sodium CMC solution at various concentrations (0.4, 0.6, and 0.8% w/v) and in Milli-Q water. All the vials were mixed and kept at room temperature, and the sedimentation height was recorded at predetermined intervals.[43]

$$F = \frac{H_u}{H_0}.$$

Syringeability testing. Syringeability is one of the critical parameters for injectable formulations, as it reflects the ease with which an injectable formulation is expelled through a syringe. Formulations that allow smooth injection are considered to have good injectability.[44] It is defined as the maximum force needed for expulsion of the formulation from the syringe, which makes it an essential factor in the evaluation of injectables.[45,46] A texture analyser (TA.XTplus) was set in compression mode, and using a 25 G gauge needle fitted on a 1 ml syringe, the prepared microspheres suspended in sodium carboxymethylcellulose solution were drawn. The parameters, including distance and a test speed of compression, were set at 40 mm and 5.00 mm s^{-1}, respectively,[47] and evaluation was done in triplicate at RT. The force required for expulsion of the formulation was recorded in newtons (N).

Residual solvent by HPLC. The acceptable levels of residual solvents are largely determined by the toxicity of the individual solvent in question. According to the ICH, the residual solvent limit depends on the toxicity of the solvent, which classifies DMSO and ethyl acetate as class 3 solvents, meaning that these solvents are less toxic and pose a lower risk to humans, and the permissible limit for DMSO and ethyl acetate is 5000 ppm.[48] Although most of the solvent evaporated overnight, residual amounts might persist. The residual amounts of ethyl acetate and DMSO were detected using HPLC. For analysis, 100 mg of microspheres were dissolved in 1 ml of acetonitrile (ACN), and 1 ml of water was then added, and the solution was centrifuged at 10 000 rpm for 5 min. The supernatant was collected and filtered through a 0.45 μm PTFE membrane and then analyzed using a Shimadzu Prominence HPLC system coupled with a Luna C18 column (250 mm × 4.60 mm, 5 μm) and an

SPD-M20A photodiode array detector. The run time was set to 15 min, the flow rate was set to 1 ml min^{-1}, and gradient elution was used.[49] The quantitation was performed at 211 nm.

Cell cytotoxicity assay. The embryonic mouse fibroblast cell line NIH 3T3 was grown in DMEM media supplemented with 10% FBS and 1% penicillin streptomycin, with 5% CO_2 at 37 °C. For the cell cytotoxicity assay, NIH 3T3 cells were grown using Dulbecco's Modified Eagle Medium (DMEM) supplemented with GlutaMax™ and high glucose (4.5 g L^{-1}). For standard growth and the cell cytotoxicity assay, the medium was supplemented with 10% (v/v) fetal bovine serum (FBS) and 1% penicillin–streptomycin (1000 U mL^{-1} penicillin and 1000 μg mL^{-1} streptomycin). Cells were cultured at 37 °C and 5% CO_2 and regularly passaged upon reaching approximately 80% confluence.[50] For the cell cytotoxicity assay, NIH 3T3 cells were seeded at a density of 3×10^3 cells per well in clear-bottom, white 96-well plates and incubated at 37 °C in a humidified atmosphere containing 5% CO_2 for 24 h to allow cell attachment. After incubation, the medium was aspirated, and cells were treated with release samples obtained from the pramipexole-loaded microsphere formulation.

Release samples were collected at two time points: 24 h and 18 days post-incubation in release medium. Each release sample was tested at its original concentration and at further dilutions of 2×, 4×, and 8× using DMEM culture media. All samples were filtered through a 0.22 μm syringe filter before cell treatment. Negative control wells contained only cell culture medium, while positive control wells contained 1% Triton X-100 in DMEM. Each treatment was performed in triplicate. Plates were incubated for an additional 24 h under the same conditions (37 °C, 5% CO_2).

Following the treatment period, cell viability was assessed using the CellTiter-Glo® 2.0 assay (Promega) according to the manufacturer's protocol. Briefly, the CellTiter-Glo reagent was added to each well, and plates were shaken for 5 min at 1000 rpm, followed by a 10 min incubation at 4 °C to stabilize the luminescence signal. Luminescence was measured as relative light units (RLU) using a Victor Nivo plate reader with an integration time of 250 ms. Cell viability (%) was calculated using the following formula.

$$\text{Cell viability}\,(\%) = \frac{\text{RLU}_{\text{treatment}} - \text{RLU}_{\text{positive control}}}{\text{RLU}_{\text{negative control}} - \text{RLU}_{\text{positive control}}} \times 100.$$

***Ex vivo* release study and *ex vivo–in vitro* correlation.** Fresh porcine hind leg muscle tissue was obtained from a local slaughterhouse within 2 hours post-mortem and transported under cold chain conditions. Muscle tissue samples were trimmed to a uniform thickness of approximately 5 × 5 cm (n = 3). 100 mg of microsphere formulation was accurately weighed and suspended in 1 mL of 0.8% sodium CMC solution and filled into a 1 mL sterile syringe with a 22 G needle. The formulation was then injected into each muscle (n = 3) and immediately transferred to a beaker containing 50 mL of PBS buffer with 0.2% sodium azide (pH 7.4). All the beakers were then transferred to an orbital shaker and incubated at 37 °C with agitation at 100 rpm to simulate physiological conditions.[51] At regular intervals (Days 2, 3, 4, 5, 6, 8, and 10), 10 mL of the release sample was collected at each time point, and 10 mL of fresh buffer was added to maintain sink conditions. The collected release samples were filtered using a 0.22 μm PTFE filter and analysed using an HPLC method. Further to establish the correlation, the *ex vivo* release study data were evaluated against the *in vitro* release profile through a linear regression model. Additionally, correlation analysis was performed using a mixed effects model with restricted maximum likelihood (REML) in GraphPad Prism (version 10.0.0). Then, pairwise comparisons between *in vitro* and *ex vivo* release at each time point were performed using Šídák's multiple comparisons test. Statistical significance was defined as $p < 0.05$.

Results and discussion

Microsphere formulation optimization

Initial microsphere formulation trials were performed using only $PLGA_{50:50}$ by the W/O/W double emulsion solvent evaporation technique. Microspheres prepared using only $PLGA_{50:50}$ at 200 mg ml^{-1} concentration showed 23% pramipexole release, followed by a very slow release, reaching only 33% in 8 days, which could be because of the hydrophobic nature of PLGA. To tune the pramipexole release, we incorporated Eudragit L-100 into the microsphere formulation. We tried different ratios of PLGA and Eudragit to evaluate their impact on the pramipexole release profile.

The combination of PLGA and Eudragit L-100 showed consistent pramipexole release for up to 8 days. Additionally, different solvents were tried for preparing microspheres, including DCM, EA, and EA : DMSO (1 : 2 ratio). The DCM microspheres showed high drug loading and encapsulation efficiency, but did not exhibit consistent drug release. The microspheres, which were prepared using EA : DMSO (1 : 2 ratio), showed low drug loading but consistent drug release. However, the dose of pramipexole is low;[52] achieving sustained drug release without a tiresome process was the aim of our study. EA : DMSO (1 : 2 ratio) was used for preparing the microspheres. Further formulation trials were performed to evaluate the effect of the oil-to-water phase ratio, PLGA concentration, and stirring speed on the drug loading and the release profile (given in Table 2).

Quantification of pramipexole using HPLC

The developed HPLC method was validated using six calibration points over a concentration range from 5 μg ml^{-1} to 100 μg ml^{-1} with three replicates (n = 3) at each concentration. The calibration curve was described by the equation $y = 22\,051x - 8932.2$, showing good linearity with an R^2 value of 0.999. The limit of detection (LOD) was found to be 2.61 μg ml^{-1}, whereas the limit of quantification (LOQ) was 7.9 μg ml^{-1}, with a retention time of 7.74 ± 0.002 min. To confirm the reliability of the developed HPLC method, accuracy and precision were evaluated and the results are presented in Tables 3 and 4. Together, these results establish the developed HPLC method as reliable and suitable for the quantification of pramipexole.

Table 2 Microsphere formulation trials prepared using the W/O/W emulsion technique

Trial	PLGA (mg ml^{-1})	Eudragit L-100 (mg ml^{-1})	O/W ratio	Stirring speed (rpm)	Drug loading	Encapsulation efficiency	Initial burst release	18 day release
F1	200	50	5	250	1.84	25.35	18.61	53.29
F2	200	50	9	450	1.23	66.18	10.3	46.90
F3	200	50	5	650	2.24	66.18	5.92	56.18
F4	200	50	1	450	1.89	15.41	13.44	53.33
F5	400	50	5	450	2.04	54.14	24.18	93.78
F6	400	50	1	250	1.42	36.88	21.42	75.63
F7	400	50	9	250	1.45	45.32	8.06	44.80
F8	400	50	9	650	1.05	60.26	7.51	61.13
F9	400	50	1	650	2.76	29.77	21.72	72.97
F10	600	50	9	450	1.33	55.98	14.72	53.24
F11	600	50	5	650	1.13	28.82	17.61	70.74
F12	600	50	5	250	0.44	37.50	8.95	53.71
F13	600	50	1	450	2.05	48.18	17.83	71.40

Table 3 Accuracy of the developed method (n = 3)

Concentration (μg ml^{-1})	% recovery ± SD
10	100.00 ± 0.01
50	99.37 ± 0.03
100	98.77 ± 0.08

Drug loading and encapsulation efficiency

The microsphere prepared using $PLGA_{50:50}$ at a 400 mg ml^{-1} concentration showed the highest drug loading and encapsulation efficiency; however, our main interest was the release profile of the drug from the prepared microspheres.

In vitro drug release

The *in vitro* drug release experiments demonstrated that only the microspheres prepared using $PLGA_{50:50}$ at a 400 mg ml^{-1} concentration with an oil phase to water phase ratio of 1 : 5 showed a consistent drug release profile, as shown in Fig. 2. An initial burst release of up to 24.18% was observed, followed by consistent release of pramipexole for up to 18 days, with an overall drug release of 93.78%. The formulation containing 600 mg ml^{-1} PLGA showed a very low burst release; however, the subsequent very slow release observed could be because of a higher concentration of the hydrophobic polymer in the microspheres.

Mathematical modelling of the drug release profile

Various mathematical models were applied to analyze the *in vitro* pramipexole release profile.[37] The experimental release data obtained for pramipexole microspheres were fitted using various models (shown in Table 5). The release profile of pramipexole was best fitted with the Peppas–Sahlin with T_{lag} and Makoid–Banakar with T_{lag} models. The Peppas–Sahlin with T_{lag} and Makoid–Banakar with T_{lag} models are represented by the equations given in Table 5.

The Peppas–Sahlin with T_{lag} model is used for describing[50] complex drug release, where drug release is due to a combination of Fickian diffusion and polymer relaxation.[53] In contrast, the Makoid–Banakar model with T_{lag} describes the release of the drug from spherical matrices,[54] and is based on the theory that the total amount of drug released is the outcome of various mechanisms, such as burst release, con-

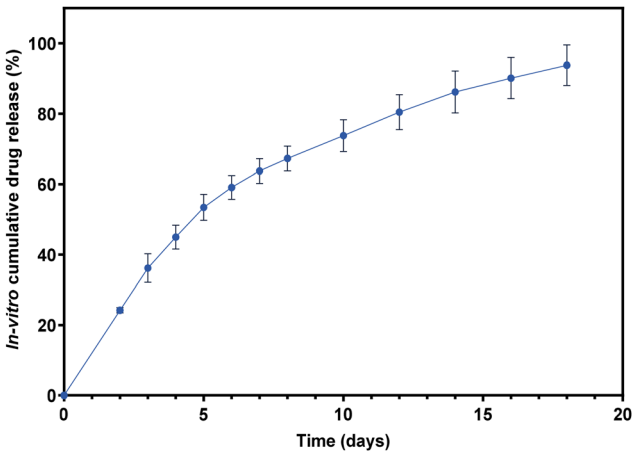

Fig. 2 The *in vitro* drug release profile of the optimized microspheres using the dialysis bag method (mean ± SEM, n = 3).

Table 4 Precision of the developed method (n = 3)

Concentration (μg ml^{-1})	% Recovery ± SD		
	Day 1 (%RSD)	Intraday (%RSD)	Day 3 (%RSD)
10	102.48 ± 0.01 (0.131)	102.07 ± 0.03 (0.331)	101.35 ± 0.02 (0.185)
50	100.08 ± 0.03 (0.069)	100.54 ± 0.12 (0.231)	100.11 ± 0.01 (0.029)
100	99.43 ± 0.04 (0.045)	99.50 ± 0.06 (0.058)	99.03 ± 0.14 (0.141)

Table 5 Mathematical modelling of pramipexole release kinetics

Model	Equation	R^2_{adj}	AIC	MSC
Zero-order with T_{lag}	$F = k_0(t - T_{lag})$	0.871	94.72	1.34
First order with T_{lag}	$F = 100[1 - \exp(-k_1(t = T_{lag}))]$	0.997	43.55	5.27
Higuchi with T_{lag}	$F = k_H(t - T_{lag})^{0.5}$	0.987	64.32	3.68
Korsmeyer–Peppas with T_{lag}	$F = \kappa_{KP}(t - T_{lag})^n$	0.998	35.83	5.87
Peppas–Sahlin with T_{lag}	$F = k_1(t - T_{lag})^m + k_2(t - T_{lag})^{2m}$	0.999	26.35	6.60
Gompertz model	$F = F_{max}\exp\{-\exp[-K(t - \gamma)]\}$	0.982	68.94	3.32
Weibull model	$F = 100\{1 - \exp[-(t - T_i)^{\beta}/\alpha]\}$	0.997	42.90	5.32
Makoid–Banakar with T_{lag}	$F = k_{MB}(t - T_{lag})^n\exp[-k(t - T_{lag})]$	0.999	26.93	6.55

trolled release, and diffusion release.[55] Based on the model fitting, we can confirm that the release of pramipexole from the microspheres is the combination of various mechanisms. The curve fitting of the *in vitro* drug release data using the Peppas–Sahlin with T_{lag} model and the Makoid–Banakar with T_{lag} model is shown in Fig. 3a and b, respectively.

Particle size distribution (PSD)

The particle size of the microspheres is crucial, particularly in the case of injectable formulations. Larger particles affect the flow of the particles through the needle, obstructing the administration of the formulation. Therefore, achieving an optimal particle size is essential for microspheres. The D_{90} for the optimized microspheres was found to be 77.1 ± 1.13 μm with a span of 1.64, demonstrating a narrow PSD (as shown in Fig. 4).

Scanning electron microscopy (SEM)

The dried optimized microsphere formulation showed a spherical shape with a wrinkled surface (Fig. 5A). However, when the microspheres were exposed to pH 7.4 phosphate buffer release medium, pores began to form on their surface by day 2 due to the diffusion of the aqueous medium. The pore size subsequently increased, as shown in Fig. 5C. Over time, the surface began to erode and degrade. As shown in Fig. 5D by day 14, the microspheres eroded significantly, which aligns with the *in vitro* release data, indicating that the release of pramipexole occurs due to a combination of different mechanisms.

Differential scanning calorimetry

Upon analysis of the DSC thermograms of pramipexole, PLGA, Eudragit L-100, and the microspheres, pure pramipexole showed a sharp endothermic peak at 129 °C, as shown in Fig. 6. However, the DSC thermogram of the microspheres showed the absence of the endothermic peak at 129 °C; only a

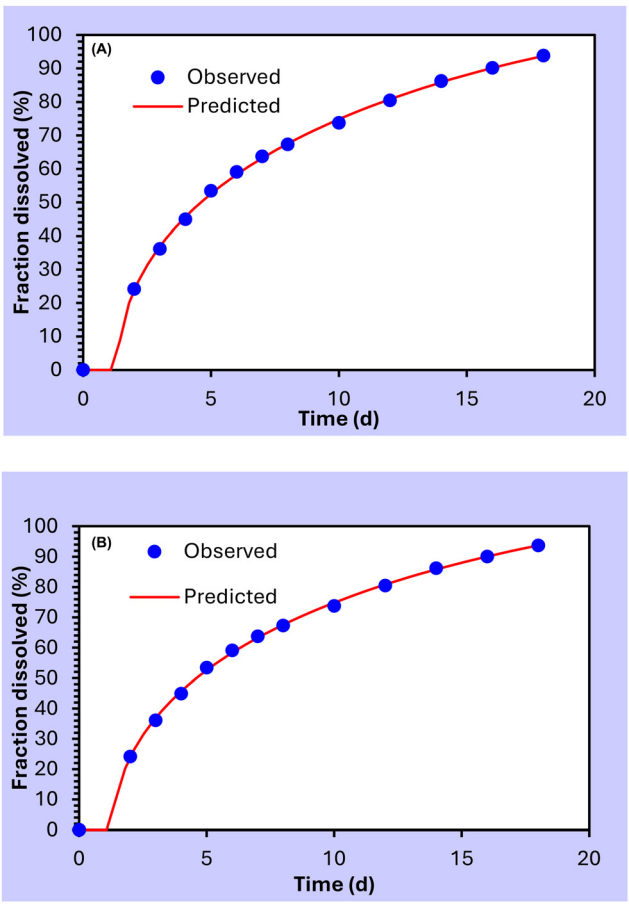

Fig. 3 (A) *In vitro* drug release data curve fitting with the Peppas–Sahlin 1 with T_{lag} model. (B) *In vitro* drug release data curve fitting with the Makoid–Banakar with T_{lag} model.

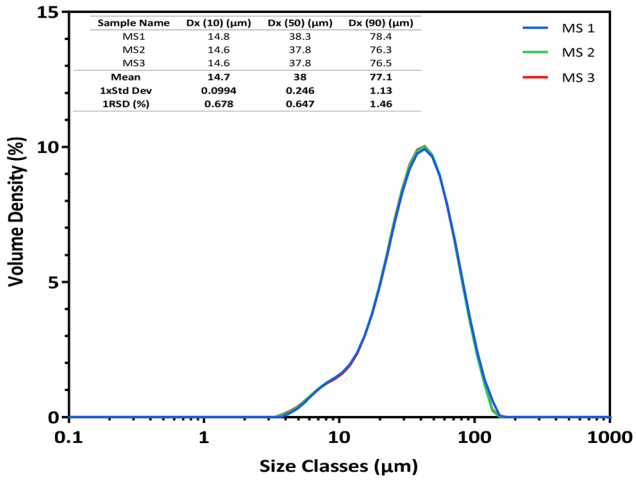

Fig. 4 Particle size distribution of microspheres determined using a Mastersizer.

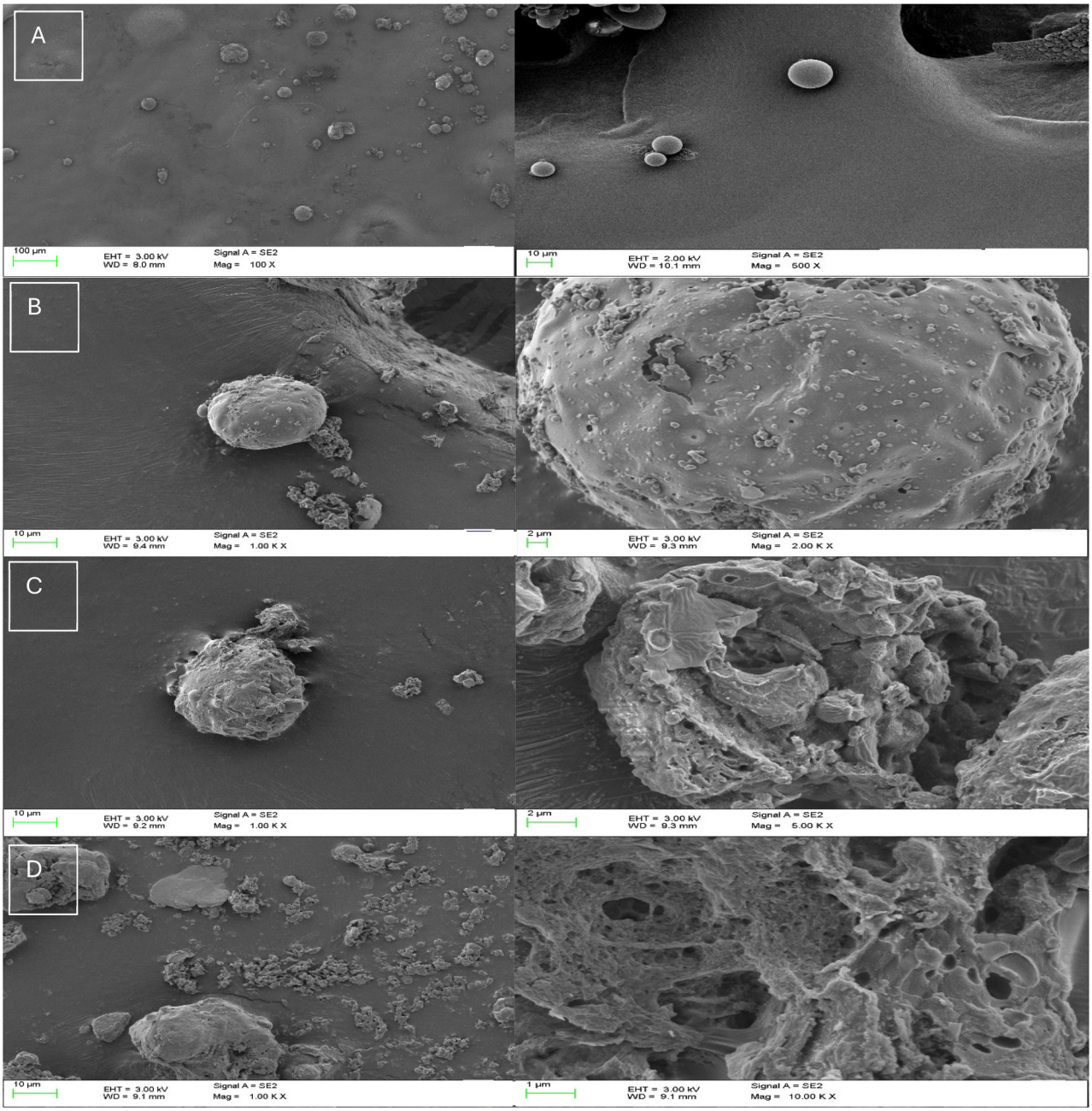

Fig. 5 SEM images of (A) lyophilized suspended microspheres, (B) Day 2 lyophilized microspheres, (C) Day 7 lyophilized microspheres, and (D) Day 14 lyophilized microspheres (images on the left are shown at a higher magnification to observe the surface morphology).

broad peak was observed at 35.86 °C, corresponding to the glass transition phase of PLGA. A degradation peak of PLGA was observed at 286 °C in the microsphere sample. The absence of the pramipexole endothermic peak indicates either the molecular dispersion of pramipexole into the PLGA microspheres or its conversion into an amorphous form.

Fourier transform infrared (FTIR) spectroscopy

Each FTIR peak is related to the specific functional groups present in the molecule; any change in the peak shape, disappearance, or shift in the peak position indicates a molecular interaction between the drug and polymer.[41] The FTIR spectra of pramipexole, PLGA, Eudragit L-100, the physical mixture, and the microspheres are presented in Fig. 7A. The peaks of interest in pramipexole were the N–H stretching vibrations observed at 3090 and 3265 cm^{-1}. These peaks disappeared in the microsphere samples, indicating the occurrence of a molecular interaction between pramipexole and the polymer. However, the C–H stretching bands of pramipexole were observed in the microspheres at 2950 and 2995 cm^{-1}. The

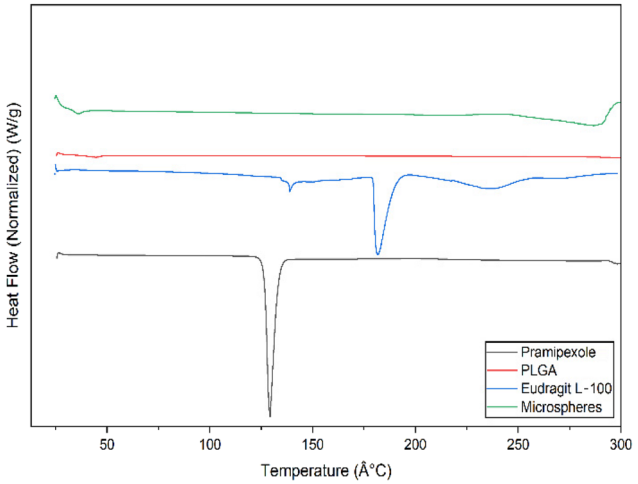

Fig. 6 DSC thermograms of pramipexole, PLGA, Eudragit L-100, and microspheres.

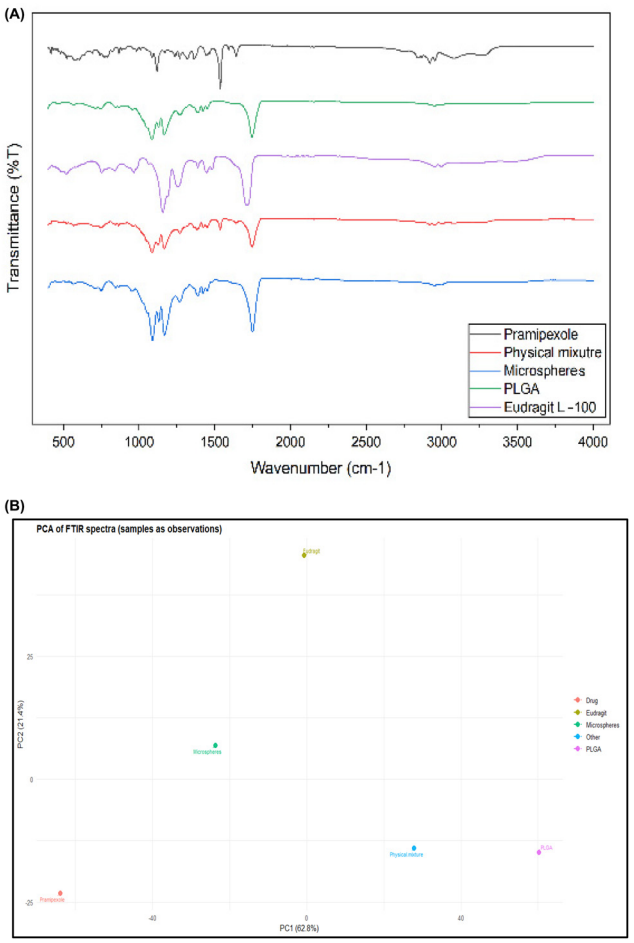

Fig. 7 (A) FTIR spectra of pramipexole, PLGA, Eudragit L-100, physical mixture, and microspheres. (B) PCA plot of FTIR spectra.

characteristic peak of PLGA was observed at 1743 cm^{-1}, while that of Eudragit L-100 was observed at 1714 cm^{-1}.[56] The higher absorption observed at 1752 cm^{-1} is due to the presence of PLGA and Eudragit in the microsphere formulation. The C–H stretching bands observed at 2950 and 2995 cm^{-1} were unlikely to be affected by the interaction between the drug and polymer.

PCA of FTIR spectra

The first three principal components together explained a substantial proportion of the total variance, with PC1 accounting for 62.82%, PC2 accounting for 21.38%, and PC3 accounting for 15.88%. Together, PC1 and PC2 explained approximately 84.2% of the variance, providing a reliable two-dimensional representation of spectral differences. The score plot demonstrated clear separation among samples: pramipexole was positioned far to the left on PC1 (−63.90) and slightly lower on PC2 (−23.22), while PLGA appeared at the far right (PC1 = +60.22; PC2 = −14.97). The physical mixture clustered near PLGA (PC1 = +27.92; PC2 = −14.12), indicating polymer-dominated characteristics, which indicates that simple blending preserves the individual spectral characteristics of the components, with no molecular interactions occurring. The microspheres occupied an intermediate position (PC1 = –23.64; PC2 = +6.81), distinct from both the pure drug and the physical mixture. This separation suggests that the formulation process altered the spectral profile of pramipexole during its incorporation into the polymer matrix, likely due to its molecular interaction with the polymer. In contrast, Eudragit was located near the origin on PC1 but exhibited a strongly positive PC2 value (PC2 = +45.50), reflecting its unique chemical contributions. Examination of the loadings shows that PC1 was primarily influenced by wavenumbers in the ~2667–2682 cm^{-1} region, which best discriminate the spectral pattern of the drug from those of PLGA and Eudragit, associated with C–H stretching and related vibrations. PC2 was driven by bands at ~1705–1715 cm^{-1} and ~1682 cm^{-1}, corresponding to carbonyl stretching typical of polymeric esters, which is consistent with the distinct ester/carbonyl environment of Eudragit's copolymer structure.

The drug and PLGA/physical mixture, although they exhibit carbonyl features, do not share the same PC2 fingerprint, underscoring Eudragit's unique spectral motif along this axis. The microspheres' intermediate PC1 position aligns with the co-presence of drug and polymer signals (encapsulation/blending), as expected for encapsulated systems. These multivariate FTIR findings align with the H^1 NMR analysis, which showed a chemical shift change of 0.15 ppm for the amine proton from δ 6.58 ppm in pure pramipexole to δ 6.73 ppm in the microspheres. This shift indicates an altered chemical environment, supporting the presence of drug–polymer interactions suggested by the distinct PCA positioning of the microspheres.

Proton NMR

The NMR spectra of pramipexole and the microsphere formulation were acquired, as shown in Fig. 8. Fig. 8(A) shows the proton NMR spectrum of pramipexole along with its chemical structure. The amine group highlighted in the red circle is the likely site of interaction between PLGA and pramipexole, and the highlighted peaks correspond to this amine group. The

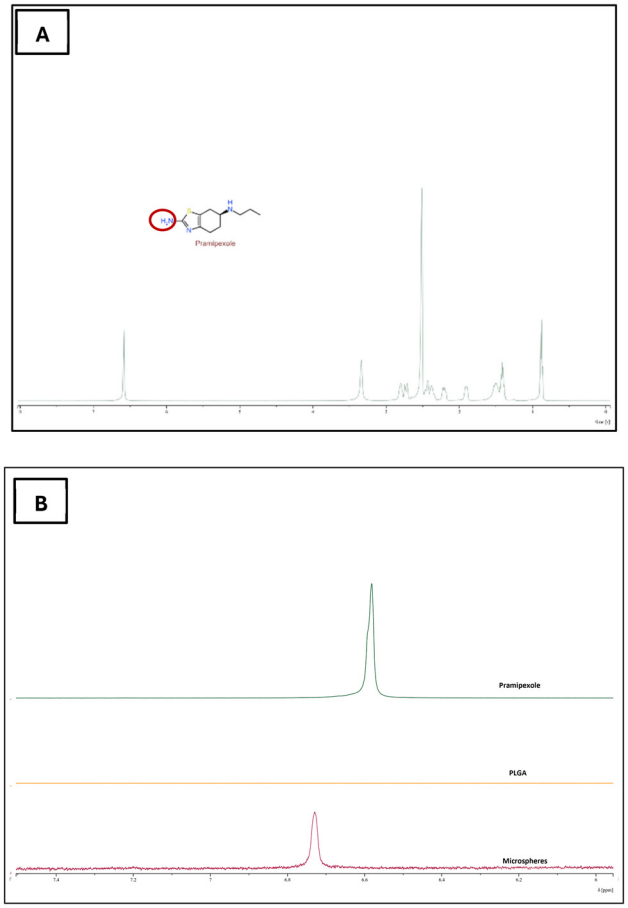

Composition	Chemical shift	Change in shift
Pramipexole	6.58	
Microspheres	6.73	0.15

Fig. 8 (A) ^{1}H NMR spectrum of pramipexole and (B) change in the chemical shift of the amine group in the presence of PLGA.

shift in the amine group of the drug (0.15 ppm) peak was identified as shown in Fig. 8(B); a significant shift was detected in the microsphere formulation (from 6.58 ppm to 6.73 ppm). This shift confirms an altered electronic environment of the amine group, identifying it as the likely site of interaction between pramipexole and PLGA.

X-Ray diffraction (XRD)

To study the crystallinity of the pramipexole microsphere formulation and also to confirm the results of the DSC and NMR studies, XRD studies were carried out. The diffractograms of the pramipexole and pramipexole-loaded microspheres are shown in Fig. 9. The diffractograms of the physical mixture were added for comparison. The diffraction pattern of the pure drug revealed several prominent peaks, indicating a high

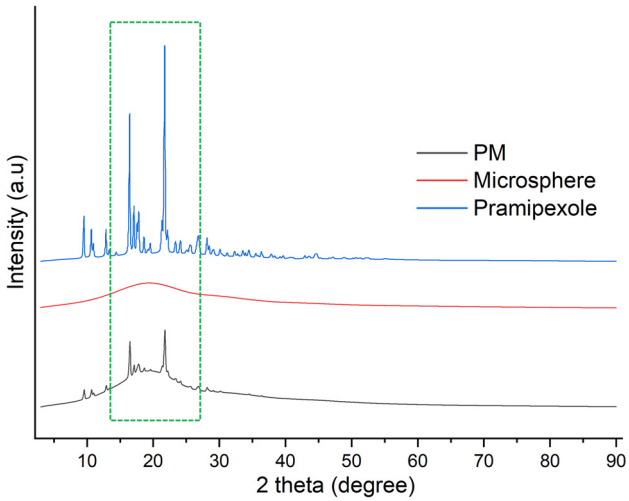

Fig. 9 X-ray diffraction patterns of pramipexole, physical mixture (PM), and pramipexole-loaded microspheres. The green rectangle highlights an area where characteristic peaks of the drug are observed.

degree of crystallinity. The diffraction pattern showed dominant peaks at 2θ values of 21.7°, 16.5°, 9.54°, 12.9°, 10.6°, 17.1°, and 17.8°, along with less intense peaks at 22.2°, 18.7°, 19.5°, 26.8°, 28.2°, 24.1° and 23.4°. The XRD pattern of the physical mixture demonstrated the crystalline peaks of pramipexole along with a broader signal attributed to the polymer. The drug-loaded microspheres showed no characteristic peaks at 2θ = 20°, which could be due to the amorphous nature of PLGA.[57] XRD indicates that the drug is homogeneously distributed throughout the polymeric matrix in an amorphous form. The XRD data, in agreement with the DSC analysis, confirmed the molecular dispersion of the drug within the microspheres.

Viscosity

Microspheres suspended in 0.8% sodium CMC were evaluated for viscosity at various shear rates to study the effect of shear rate on viscosity. The sample was subjected to different shear rates from 100 to 2000, as shown in Fig. 10. The viscosity results show the shear-thinning (pseudoplastic) behaviour of the microsphere suspension.[58] Once the shear stress was stopped, the viscosity returned to its original value. The lower viscosity of the suspension is an indicator of good injectability of the formulation, which was confirmed by the syringeability test.

Suspending test

When microspheres were suspended in water, rapid settling was observed compared with suspensions prepared using sodium CMC, increasing the risk of caking due to compact sediment formation. In contrast, when microspheres were suspended in sodium CMC, with the increasing concentration of sodium CMC, slowing down of the particle settling was observed, as shown in Fig. 11. Sodium CMC at 0.8% con-

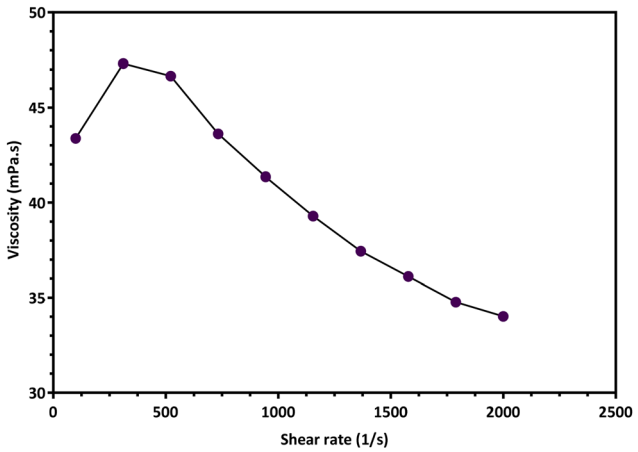

Fig. 10 Effect of shear rate on the viscosity of the suspended microspheres at 37 °C.

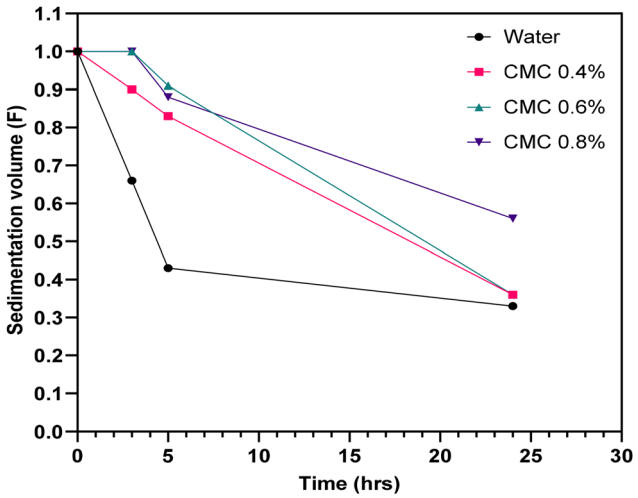

Fig. 11 Sedimentation behaviour of the microspheres at room temperature.

centration showed lower sedimentation with a larger final sediment volume; hence, 0.8% CMC concentration was selected for suspending the microspheres for injectable administration.

Syringeability testing

The ejection force observed for the microspheres when suspended in the 0.8% CMC solution at 50 mg ml^{-1} concentration, using a 25-gauge needle, was found to be 3.25 ± 0.24 N at room temperature. However, the force required for ejection of 3.25 N indicates the ease of injection of the formulation without causing pain.[46]

Residual solvent content

The results demonstrated that the amount of DMSO present in 100 mg of microspheres was 1.83 ppm, whereas for ethyl acetate, the amount was below 25 ppm, which was below the lowest limit of quantitation of the developed HPLC method. The residual DMSO and ethyl acetate present in the microspheres were within the permissible limit of 5000 ppm specified by ICH guidelines.

Cell cytotoxicity assay

The cytotoxicity of pramipexole released from the microsphere formulation was evaluated at two time points: 24 hours and 18 days post-incubation. Cell viability was assessed after treating NIH 3T3 fibroblast cells with the release samples and their corresponding dilutions.

For the 24 hour release sample (Fig. 12A), cell viability decreased in a concentration-dependent manner. At the highest tested concentration (26 µg mL^{-1}), cell viability was

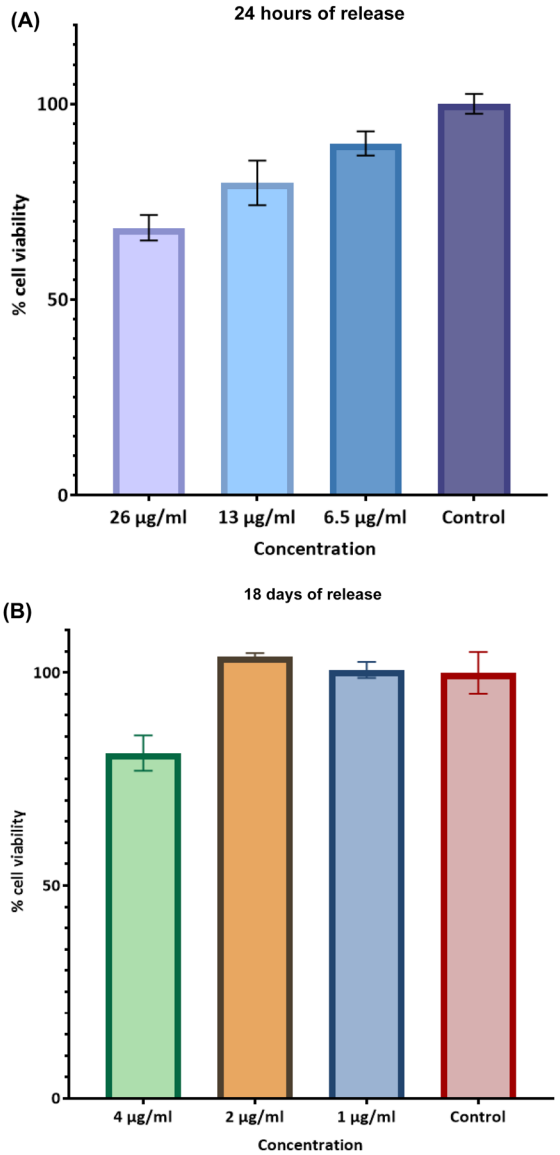

Fig. 12 (A) *In vitro* cell viability results of the formulation at 24 hours of release using 3T3 cell lines. (B). *In vitro* cell viability results of the formulation at 18 days of release using 3T3 cell lines.

approximately 65%, indicating moderate cytotoxicity. At 13 μg mL^{-1}, cell viability improved to around 80%, and at 6.5 μg mL^{-1}, it reached nearly 90%, comparable to the control group (≈100%). These results suggest that the initial burst release from the microspheres may exert a measurable cytotoxic effect at higher concentrations.

In contrast, the 18 day release sample (Fig. 12B) exhibited minimal cytotoxicity across all tested concentrations. At 4 μg mL^{-1}, cell viability remained above 85%, while at 2 μg mL^{-1} and 1 μg mL^{-1}, it was approximately 100%, similar to that of the control group. This indicates that the prolonged release phase of the microspheres delivers the drug at concentrations that are well tolerated by fibroblast cells.

Overall, the 24 hour release sample showed moderate cytotoxicity at higher concentrations, likely due to the initial burst release of the drug, which is commonly observed in microsphere systems. However, even at the highest concentration tested (26 μg mL^{-1}), cell viability remained above 60%, suggesting that the formulation does not induce severe toxicity.

By day 18, the release profile shifted to a sustained, lower concentration drug delivery pattern, resulting in negligible cytotoxicity across all tested dilutions. This sustained release behaviour is desirable for long-term therapeutic applications, as it minimises the risk of local toxicity while maintaining drug availability.

Overall, these findings indicate that the microsphere formulation enabled a controlled release of the drug, with an initial burst followed by a stable, non-toxic release phase. This release pattern could be advantageous for achieving therapeutic efficacy while reducing adverse effects associated with high local drug concentrations.

Ex vivo drug release and *ex vivo–in vitro* correlation

The cumulative release profile of pramipexole from microspheres under *in vitro* and *ex vivo* conditions was compared over 10 days. As shown in Fig. 13, both release curves show a sustained release of the drug up to 75–80% by day 10. However, notable differences were observed between the two conditions. The *ex vivo* release profile of pramipexole demonstrated a consistently ~10% higher cumulative drug release on days 2, 3, and 4 compared to the *in vitro* profile. This enhanced release is likely driven by tissue-specific factors such as enzymatic activity, hydration, and localised diffusion within the pig muscle matrix. By day 10, both systems achieved a sustained cumulative drug release of 75 ± 5%. The *ex vivo* study was terminated on day 10 due to observable tissue degradation, which compromised sample integrity. Despite this limitation, the data suggest that microsphere formulation is capable of enabling sustained release for up to 18 days, as demonstrated *in vitro*.

To further evaluate the predictive relationship between *in vitro* and *ex vivo* drug release profiles, linear regression analysis was performed using GraphPad (version 10.0.0).[59] The cumulative percentage of pramipexole released under *ex vivo* conditions was plotted against the corresponding *in vitro* release values across each time point, as shown in Fig. 14. The

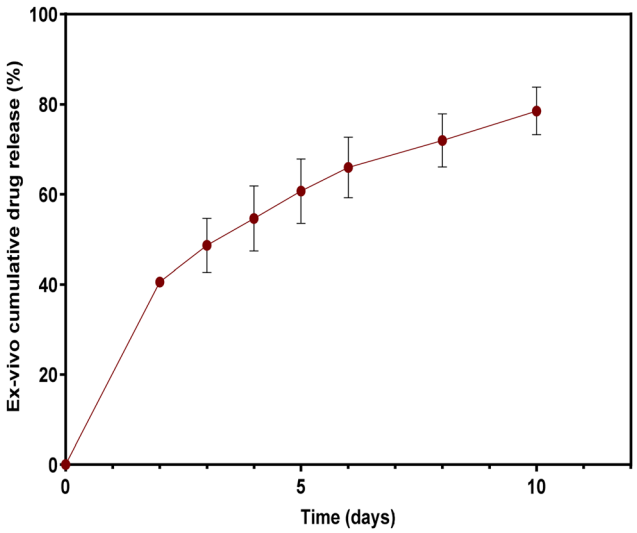

Fig. 13 Cumulative *ex vivo* drug release profile of pramipexole microspheres.

resulting regression equation was $y = 0.968–6.0758$ with a coefficient of determination (R^2) of 0.9574, indicating a strong linear correlation. Furthermore, the comparison of the *in vitro* and *ex vivo* release profiles at matched time points showed no statistically significant difference ($p = 0.1372$), demonstrating strong similarity between the two datasets and suggesting that the *in vitro* release behaviour reliably reflects *ex vivo* performance. These findings support the validity of the *in vitro* system as a replacement for *in vivo* pharmacokinetic performance while highlighting the importance of the *ex vivo* model in capturing physiological conditions. This strong correlation emphasises the reliability of the formulation and its potential for predictable *in vivo* performance.

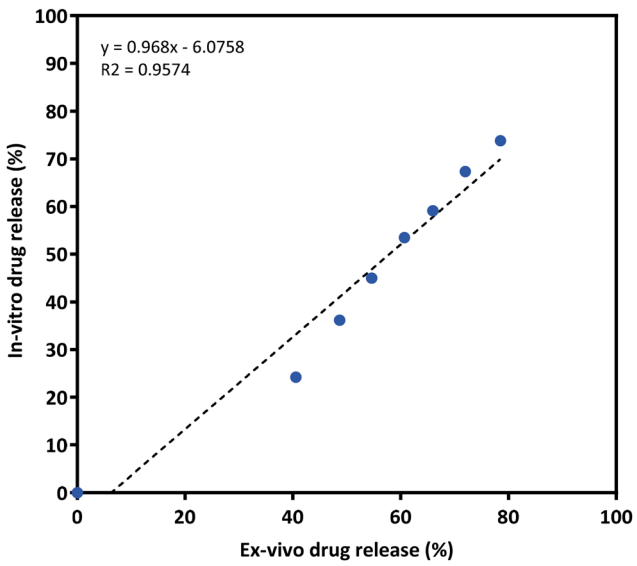

Fig. 14 *Ex vivo–in vitro* correlation between the drug release profiles.

Conclusion

This study reports the formulation of biodegradable microspheres for sustained release of pramipexole. For the first time, PLGA and Eudragit L-100 were used in combination to exploit the advantages of both polymers for tuning the drug release. PLGA helps in controlling drug release, whereas pH-specific dissolution of Eudragit-L 100 aids in achieving consistent pramipexole release. The *in vitro* drug release profile of pramipexole showed sustained release for up to 18 days using the dialysis bag method. The developed microspheres were evaluated for the interaction between pramipexole and PLGA by NMR and FTIR. The microspheres showed a uniform particle size distribution when evaluated using a Mastersizer. The microspheres were further suspended in sodium CMC solution, and the microspheres were evaluated for syringeability. The injection force for microspheres was found to be 3.25 ± 0.24 N, which shows an easy-to-inject formulation. The results from *ex vivo* drug release studies showed a good correlation between the *in vitro* drug release and *ex vivo* drug release profiles, with a correlation coefficient of 0.95. Therefore, the developed microspheres can enable the sustained release of pramipexole without the need for conversion into a salt form. However, future studies should include *in vivo* pharmacokinetic and pharmacodynamic evaluations of the pramipexole-loaded microspheres to confirm their sustained-release behaviour and therapeutic efficacy in relevant animal models. Long-term stability studies, scale-up, manufacturing feasibility, and comprehensive assessment of the biocompatibility and safety of the polymer combination will be essential to support the clinical translation of the proposed formulation. In addition, systematic optimization of the PLGA/Eudragit L-100 and microsphere suspension vehicle may enable fine-tuning of the release profile for different dosing intervals and patient needs, ultimately enhancing patient adherence in Parkinson's disease management.

Author contributions

Deepa Nakmode: conceptualization, methodology, data curation, formal analysis, investigation, writing – original draft, and visualization. Haripriya Koppisetti: methodology and writing – review & editing. Weranga Rajapaksha: formal analysis and writing – review & editing. Yunmei Song: conceptualization, writing – review & editing, supervision, and project administration. Sanjay Garg: conceptualization, resources, writing – review & editing, supervision, project administration, and funding acquisition.

Conflicts of interest

The authors declare no conflicts of interest.

Data availability

The data supporting this article have been included as part of the supplementary information (SI). Supplementary information: pramipexole HPLC validation details. See DOI: https://doi.org/10.1039/d6pm00029k.

Acknowledgements

The authors acknowledge the use of the facilities and scientific and technical assistance of Microscopy Australia at the University of South Australia, a facility that is co-funded by the University of South Australia and the state and federal governments. We thank Professor Volker Hessel and Rabin Duwal for their support with the XRD experiments at the University of Adelaide Analytical Laboratorys.

References

1 M. Rezak, Current pharmacotherapeutic treatment options in Parkinson's disease, *Dis. Mon.*, 2007, **53**(4), 214–222.
2 A. H. Rajput, W. Martin, M. H. Saint-Hilaire, E. Dorflinger and S. Pedder, Tolcapone improves motor function in parkinsonian patients with the "wearing-off" phenomenon: a double-blind, placebo-controlled, multicenter trial, *Neurology*, 1998, **50**(5 Suppl 5), S54–S59.
3 A. Antonini, P. Barone, R. Ceravolo, G. Fabbrini, M. Tinazzi and G. Abbruzzese, Role of pramipexole in the management of Parkinson's disease, *CNS Drugs*, 2010, **24**(10), 829–841.
4 R. A. Hauser, A. H. Schapira, O. Rascol, P. Barone, Y. Mizuno, L. Salin, *et al.*, Randomized, double-blind, multicenter evaluation of pramipexole extended release once daily in early Parkinson's disease, *Mov. Disord.*, 2010, **25**(15), 2542–2549.
5 J. P. Jr. Bennett and M. F. Piercey, Pramipexole–a new dopamine agonist for the treatment of Parkinson's disease, *J. Neurol. Sci.*, 1999, **163**(1), 25–31.
6 S. M. Wilson, M. G. Wurst, M. F. Whatley and R. N. Daniels, Classics in Chemical Neuroscience: Pramipexole, *ACS Chem. Neurosci.*, 2020, **11**(17), 2506–2512.
7 B. S. Connolly and A. E. Lang, Pharmacological treatment of Parkinson disease: a review, *J. Am. Med. Assoc.*, 2014, **311**(16), 1670–1683.
8 K. M. Biglan and R. G. Holloway, A review of pramipexole and its clinical utility in Parkinson's disease, *Expert Opin. Pharmacother.*, 2002, **3**(2), 197–210.
9 J. Maj, Z. Rogoi, W. Margas, M. Kata and M. Dziedzicka-Wasylewska, The effect of repeated treatment with pramipexole on the central dopamine D3 system, *J. Neural Transm.*, 2000, **107**(12), 1369–1379.
10 A. Antonini and D. Calandrella, Pharmacokinetic evaluation of pramipexole, *Expert Opin. Drug Metab. Toxicol.*, 2011, **7**(10), 1307–1314.

11 P. Jenner, M. Konen-Bergmann, C. Schepers and S. Haertter, Pharmacokinetics of a once-daily extended-release formulation of pramipexole in healthy male volunteers: three studies, *Clin. Ther.*, 2009, **31**(11), 2698–2711.
12 S. Perez-Lloret, M. V. Rey, L. Ratti and O. Rascol, Pramipexole for the treatment of early Parkinson's disease, *Expert Rev. Neurother.*, 2011, **11**(7), 925–935.
13 J. P. Hubble, Pre-clinical studies of pramipexole: clinical relevance, *Eur. J. Neurol.*, 2000, **7**(Suppl 1), 15–20.
14 I. Suttrup and T. Warnecke, Dysphagia in Parkinson's Disease, *Dysphagia*, 2016, **31**(1), 24–32.
15 A. Bauer, P. Berben, S. S. Chakravarthi, S. Chattorraj, A. Garg, B. Gourdon, *et al.*, Current State and Opportunities with Long-acting Injectables: Industry Perspectives from the Innovation and Quality Consortium "Long-Acting Injectables", *Work. Group Pharm. Res.*, 2023, **40**(7), 1601–1631.
16 W. Jiang and S. P. Schwendeman, Stabilization of a model formalinized protein antigen encapsulated in poly(lactide-co-glycolide)-based microspheres, *J. Pharm. Sci.*, 2001, **90**(10), 1558–1569.
17 F. Molavi, M. Barzegar-Jalali and H. Hamishehkar, Polyester based polymeric nano and microparticles for pharmaceutical purposes: A review on formulation approaches, *J. Controlled Release*, 2020, **320**, 265–282.
18 M. Thing, C. Larsen, J. Ostergaard, H. Jensen and S. W. Larsen, In vitro release from oil injectables for intra-articular administration: Importance of interfacial area, diffusivity and partitioning, *Eur. J. Pharm. Sci.*, 2012, **45**(3), 351–357.
19 S. Alidori, R. Subramanian and R. Holm, Patient-Centric Long-Acting Injectable and Implantable Platforms horizontal line An Industrial Perspective, *Mol. Pharm.*, 2024, **21**(9), 4238–4258.
20 M. Parent, C. Nouvel, M. Koerber, A. Sapin, P. Maincent and A. Boudier, PLGA in situ implants formed by phase inversion: critical physicochemical parameters to modulate drug release, *J. Controlled Release*, 2013, **172**(1), 292–304.
21 S. Kempe and K. Mader, In situ forming implants - an attractive formulation principle for parenteral depot formulations, *J. Controlled Release*, 2012, **161**(2), 668–679.
22 M. J. Ho, M. Y. Jeong, H. T. Jeong, M. S. Kim, H. J. Park, D. Y. Kim, *et al.*, Effect of particle size on in vivo performances of long-acting injectable drug suspension, *J. Controlled Release*, 2022, **341**, 533–547.
23 M. C. Chen, S. F. Huang, K. Y. Lai and M. H. Ling, Fully embeddable chitosan microneedles as a sustained release depot for intradermal vaccination, *Biomaterials*, 2013, **34**(12), 3077–3086.
24 M. Gunawardana, M. Remedios-Chan, C. S. Miller, R. Fanter, F. Yang, M. A. Marzinke, *et al.*, Pharmacokinetics of long-acting tenofovir alafenamide (GS-7340) subdermal implant for HIV prophylaxis, *Antimicrob. Agents Chemother.*, 2015, **59**(7), 3913–3919.
25 D. D. Nakmode, S. Abdella, Y. Song and S. Garg, Development of an *in situ* forming implant system for levodopa and carbidopa for the treatment of parkinson's disease, *Drug Deliv. Transl. Res.*, 2025, **15**, 4026–4042.
26 C. I. Nkanga, A. Fisch, M. Rad-Malekshahi, M. D. Romic, B. Kittel, T. Ullrich, *et al.*, Clinically established biodegradable long acting injectables: An industry perspective, *Adv. Drug Delivery Rev.*, 2020, **167**, 19–46.
27 F. Ramazani, W. Chen, C. F. van Nostrum, G. Storm, F. Kiessling, T. Lammers, *et al.*, Strategies for encapsulation of small hydrophilic and amphiphilic drugs in PLGA microspheres: State-of-the-art and challenges, *Int. J. Pharm.*, 2016, **499**(1–2), 358–367.
28 S. Freitas, H. P. Merkle and B. Gander, Microencapsulation by solvent extraction/evaporation: reviewing the state of the art of microsphere preparation process technology, *J. Controlled Release*, 2005, **102**(2), 313–332.
29 J. Lee, H. J. Kwon, H. Ji, S. H. Cho, E. H. Cho, H. D. Han, *et al.*, Marbofloxacin-encapsulated microparticles provide sustained drug release for treatment of veterinary diseases, *Mater. Sci. Eng., C*, 2016, **60**, 511–517.
30 R. Raj, S. Wairkar, V. Sridhar and R. Gaud, Pramipexole dihydrochloride loaded chitosan nanoparticles for nose to brain delivery: Development, characterization and in vivo anti-Parkinson activity, *Int. J. Biol. Macromol.*, 2018, **109**, 27–35.
31 K. Pamlenyi, G. Jr. Regdon, O. Jojart-Laczkovich, D. Nemes, I. Bacskay and K. Kristo, Formulation and characterization of pramipexole containing buccal films for using in Parkinson's disease, *Eur. J. Pharm. Sci.*, 2023, **187**, 106491.
32 S. Li, J. Liu, G. Li, X. Zhang, F. Xu, Z. Fu, *et al.*, Near-infrared light-responsive, pramipexole-loaded biodegradable PLGA microspheres for therapeutic use in Parkinson's disease, *Eur. J. Pharm. Biopharm.*, 2019, **141**, 1–11.
33 Q. Ban, L. Zhang, J. Yan, J. Wang, T. Li and S. Liu, Engineered poly (lactide-co-glycolide) microspheres for sustained and uniform release of pramipexole xinafoate to maintain long-term stable blood drug levels, *J. Drug Deliv. Sci. Technol.*, 2025, 107324.
34 . Available from: https://www.merckmillipore.com/deepweb/assets/sigmaaldrich/product/documents/252/744/0009-pharmacopoeia-monograph-methods-pramipexole-mk.pdf.
35 M. A. Momoh, F. C. Kenechukwu and A. A. Attama, Formulation and evaluation of novel solid lipid microparticles as a sustained release system for the delivery of metformin hydrochloride, *Drug Delivery*, 2013, **20**(3–4), 102–111.
36 S. Amatya, E. J. Park, J. H. Park, J. S. Kim, E. Seol, H. Lee, *et al.*, Drug release testing methods of polymeric particulate drug formulations, *J. Pharm. Invest.*, 2013, **43**(4), 259–266.
37 T. Ojstersek, F. Vrecer and G. Hudovornik, Comparative Fitting of Mathematical Models to Carvedilol Release Profiles Obtained from Hypromellose Matrix Tablets, *Pharmaceutics*, 2024, **16**(4), 498.
38 S. Chaurasia, K. Mounika, V. Bakshi and V. Prasad, 3-month parenteral PLGA microsphere formulations of risperidone: Fabrication, characterization and neuropharmacological assessments, *Mater. Sci. Eng., C*, 2017, **75**, 1496–1505.

39 S. Chelouche, D. Trache, R. Benlemir and A. Soudani, Principal component analysis of FTIR data to accurately assess the real/equivalent in-service-times of homogenous solid propellant, *Propellants, Explos., Pyrotech.*, 2022, **47**(6), e202100352.
40 A. Banas, K. Banas, S. K. Lim, J. Loke and M. Breese, Broad Range FTIR Spectroscopy and Multivariate Statistics for High Energetic Materials Discrimination, *Anal. Chem.*, 2020, **92**(7), 4788–4797.
41 P. Joshi, P. Mallepogu, H. Kaur, R. Singh, I. Sodhi, S. K. Samal, *et al.*, Explicating the molecular level drug-polymer interactions at the interface of supersaturated solution of the model drug: Albendazole, *Eur. J. Pharm. Sci.*, 2021, **167**, 106014.
42 U. C. Oz, B. Devrim, A. Bozkir and K. Canefe, Development of reconstitutable suspensions containing diclofenac sodium-loaded microspheres for pediatric delivery, *J. Microencapsul.*, 2015, **32**(4), 317–328.
43 A. K. Tiwary and G. M. Panpalia, Influence of crystal habit on trimethoprim suspension formulation, *Pharm. Res.*, 1999, **16**(2), 261–265.
44 S. Dawre, S. Pathak, S. Sharma and P. V. Devarajan, Enhanced antimalalarial activity of a prolonged release in situ gel of arteether-lumefantrine in a murine model, *Eur. J. Pharm. Biopharm.*, 2018, **123**, 95–107.
45 R. Sheshala, G. C. Hong, W. P. Yee, V. S. Meka and R. R. S. Thakur, In situ forming phase-inversion implants for sustained ocular delivery of triamcinolone acetonide, *Drug Deliv. Transl. Res.*, 2019, **9**(2), 534–542.
46 W. Rungseevijitprapa and R. Bodmeier, Injectability of biodegradable in situ forming microparticle systems (ISM), *Eur. J. Pharm. Sci.*, 2009, **36**(4–5), 524–531.
47 Y. Song, S. Abdella, F. Afinjuomo, E. J. Weir, J. Q. E. Tan, P. Hill, *et al.*, Physicochemical properties of otic products for Canine Otitis Externa: comparative analysis of marketed products, *BMC Vet. Res.*, 2023, **19**(1), 39.
48 . ICH. ICH HARMONISED GUIDELINE, IMPURITIES: GUIDELINE FOR RESIDUAL SOLVENTS Q3C(R6): ICH; 2019 [Available from: https://database.ich.org/sites/default/files/Q3C-R6_Guideline_ErrorCorrection_2019_0410_0.pdf].
49 D. D. Nakmode, S. H. Youssef, S. Das, Y. Song and S. Garg, Analytical method for simultaneous quantification of levodopa and carbidopa in the injectable oleogel formulation by HPLC, *BMC Chem.*, 2025, **19**(1), 1–14.
50 A. M. Rahimi, M. Cai and S. Hoyer-Fender, Heterogeneity of the NIH3T3 Fibroblast Cell Line, *Cells*, 2022, **11**(17), 2677.
51 D. D. Nakmode, S. Abdella, Y. Song and S. Garg, Development of an *in situ* forming implant system for levodopa and carbidopa for the treatment of parkinson's disease, *Drug Deliv. Transl. Res.*, 2025, 1–17.
52 . Drugs.com. Pramipexole Dosage 2025, [Available from: https://www.drugs.com/dosage/pramipexole.html].
53 O. Y. Mady and A. A. Donia, A new mathematic method for calculation of peppas-sahli n model constants and interpret the results in relation to zero order, higuchi, korsmeyer-peppas models and microcapsule structure image, *World J. Pharm. Res.*, 2015, **4**, 2199–2246.
54 D. Ramyadevi and K. Rajan, Interaction and release kinetics study of hybrid polymer blend nanoparticles for pH independent controlled release of an anti-viral drug, *J. Taiwan Inst. Chem. Eng.*, 2015, **50**, 1–11.
55 S. A. Ward, R. N. Kirkwood, K. J. Plush, S. Abdella, Y. Song and S. Garg, Development of a Novel Vaginal Drug Delivery System to Control Time of Farrowing and Allow Supervision of Piglet Delivery, *Pharmaceutics*, 2022, **14**(2), 340.
56 S. H. Youssef, S. Kim, R. Khetan, F. Afinjuomo, Y. Song and S. Garg, The development of 5-fluorouracil biodegradable implants: A comparative study of PCL/PLGA blends, *J. Drug Deliv. Sci. Technol.*, 2023, **81**, 104300.
57 P. Gentile, V. Chiono, I. Carmagnola and P. V. Hatton, An overview of poly(lactic-co-glycolic) acid (PLGA)-based biomaterials for bone tissue engineering, *Int. J. Mol. Sci.*, 2014, **15**(3), 3640–3659.
58 X. H. Yang and W. L. Zhu, Viscosity properties of sodium carboxymethylcellulose solutions, *Cellulose*, 2007, **14**(5), 409–417.
59 Q. Bao, B. Newman, Y. Wang, S. Choi and D. J. Burgess, In vitro and ex vivo correlation of drug release from ophthalmic ointments, *J. Controlled Release*, 2018, **276**, 93–101.